

## Strong electron confinement by stacking-fault-induced fractional steps on Ag(111) surfaces

Takashi Uchihashi,<sup>1,\*</sup> Katsuyoshi Kobayashi,<sup>2</sup> and Tomonobu Nakayama<sup>1</sup><sup>1</sup>International Center for Materials Nanoarchitectonics, National Institute for Materials Science, 1-1 Namiki, Tsukuba 305-0044, Japan<sup>2</sup>Department of Physics, Faculty of Science, Ochanomizu University, 2-1-1 Otsuka, Bunkyo-ku, Tokyo 112-8610, Japan

(Received 19 July 2010; published 29 September 2010)

The electron-reflection amplitude  $R$  at stacking-fault- (SF-) induced fractional steps is determined for Ag(111) surface states using a low-temperature scanning tunneling microscope. Unexpectedly,  $R$  remains as high as 0.6–0.7 as energy increases from 0 to 0.5 eV, which is in clear contrast to its rapidly decreasing behavior for monatomic steps [L. Bürgi *et al.*, *Phys. Rev. Lett.* **81**, 5370 (1998)]. Tight-binding calculations based on *ab initio* derived band structures confirm the experimental finding. The result may be explained by a significant contribution of the subsurface SF plane to the reflection of surface states.

DOI: 10.1103/PhysRevB.82.113413

PACS number(s): 73.20.At, 73.22.Dj, 73.61.At

The Shockley surface states on a noble metal exemplify an ideal two-dimensional electron system, which works as a basis for demonstrating and utilizing quantum natures of electrons.<sup>1–3</sup> Confinement of the surface states into a lower dimension is of particular interest due to its potential applications to the nanoscale engineering, e.g., self-assembling of atoms<sup>4,5</sup> and spatial modulation of plasmonic light emission.<sup>6</sup> To realize such a quantum confinement, monatomic (MA) steps,<sup>7–12</sup> artificially manipulated atoms,<sup>13,14</sup> and self-assembled molecules<sup>5</sup> have successfully been used. However, the lifetimes of resultant quantized states are rather short especially at high energies, because of lossy scattering at the boundary caused by low reflection amplitude.<sup>15–18</sup> This may pose a fundamental limitation on the usage of these quantum structures. Although the reflection at the boundary may be enhanced by multiplying potential barriers,<sup>19</sup> a search for a new form of confinement is highly desirable. Recently, stacking-fault (SF) defects have been found to substantially modify surface and bulk electronic states of Ag thin films.<sup>20–23</sup> Nevertheless, basic properties concerning the reflection of surface states by a SF-induced step have so far remained elusive.

In this paper, we determine the reflection amplitude  $R$  at SF steps for Ag(111) surface states using a low-temperature scanning tunneling microscope (STM).  $R$  retains high values of 0.6–0.7 as energy increases from 0 to 0.5 eV, which is in striking contrast to the rapid decrease in  $R$  for MA steps reported in Ref. 9. Tight-binding calculations based on *ab initio* derived band structures confirm the experimental finding. These results demonstrate that SF steps offer a better method for realizing a strong quantum confinement on metal surfaces than MA steps. A possibility of significant scattering of the surface state by the subsurface SF plane is proposed to explain the results.

The experiments were performed in an ultrahigh vacuum system equipped with a low-temperature STM. To determine the reflection amplitude, sufficiently long and straight SF steps are needed. For this aim, Si(111)-(4×1)-In surfaces (referred to as In 4×1) were used as atomic-scale geometric templates.<sup>20,21,24</sup> Ag films about 20 monolayers (MLs) in thickness were grown on In 4×1 around 100 K followed by a natural annealing to room temperature. This results in penetration of high-density SF planes into the film, which are terminated by “fractional” steps with a height of 0.078 nm

(equivalent to 1/3 of the MA step height).<sup>24</sup> Figures 1(a) and 1(b) show a typical STM image of a Ag(111) film with SF step arrays and a tilt-corrected height profile taken along the dashed line ( $z$ : height,  $x$ : lateral distance). Although the measured step heights have an uncertainty of  $\pm 20\%$  around the expected value of 0.078 nm, they are clearly different from those of MA steps (0.22–0.25 nm). Thus they can be safely attributed to SF steps. In the present study, partially ordered triple-domain In 4×1 surfaces were used as substrates. This allowed us to have relatively wide terraces where SF-bounded triangles and MA-bounded hexagons were created, as shown later.

All STM measurements were performed below 8 K. Sample bias voltages  $V$  were measured relative to the tip. Differential conductance ( $dI/dV$ ) spectra were acquired by standard lock-in ac detection with a modulation amplitude  $V_{\text{mod}}$  of 2 mV<sub>p-p</sub>–10 mV<sub>p-p</sub>.  $dI/dV$  images were taken with  $V_{\text{mod}}=10$  mV<sub>p-p</sub>–40 mV<sub>p-p</sub> while scanning in the constant current mode. Theoretical calculations of reflection amplitudes were performed using a tight-binding method, where the tight-binding parameters were determined to reproduce a band structure of a Ag(111) thin film obtained by a density-functional method. The structure model shown in Fig. 1(a) was used for the stacking-fault structure. Details of calculation methods have been described previously.<sup>23</sup> In the present paper we used a slab of ten layers, which is sufficient to discuss the surface state. To be compared with experimental results, reflection probability was averaged over the one-

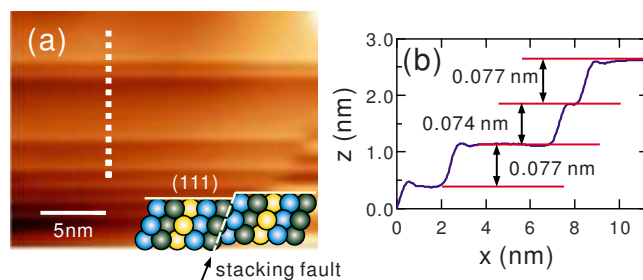


FIG. 1. (Color online) (a) Typical topographic STM image of a Ag(111) film with SF-induced fractional steps ( $V=+1.0$  V). Inset: schematic of the atomic structure of a Ag(111) film with a SF defect. (b) Tilt-corrected height profile taken along the dashed line in (a) ( $z$ : height,  $x$ : lateral distance).

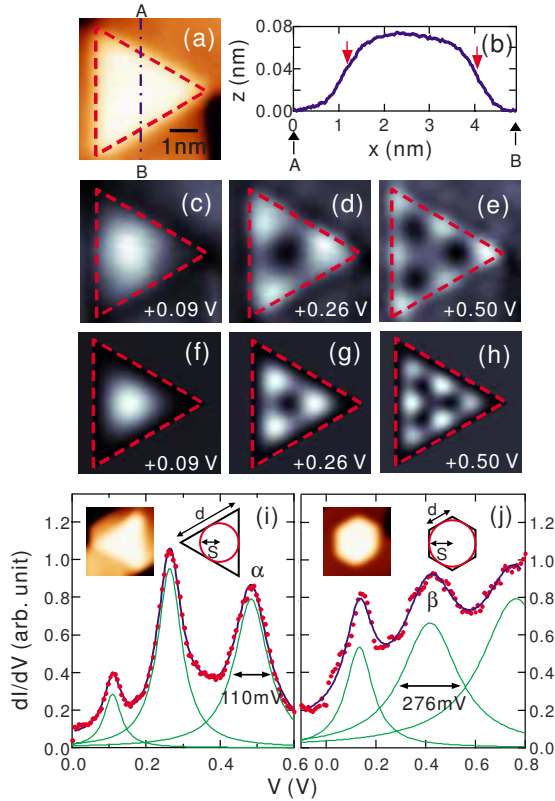


FIG. 2. (Color online) (a) Topographic STM image of a SF-bounded equilateral triangle island ( $V=-2$  V). (b) Height profile taken along the line A-B indicated in (a). [(c)–(e)] Series of  $dI/dV$  images taken on the triangle island in (a). [(f)–(h)] Simulated  $dI/dV$  images for the same triangle island. Dots:  $dI/dV$  spectra taken on (i) a SF-bounded equilateral triangle island and (j) a MA step-bounded hexagonal island. Purple (dark gray) lines: fitting results using multiple Lorentzian functions. Green (light gray) lines: components of the Lorentzian functions. Inset: STM images and their schematic illustrations of the islands.

dimensional (1D) Brillouin zone in the direction parallel to the step line.

Figure 2(a) shows a representative topographic image of a triangular island bounded by SF steps obtained at  $V=-2$  V. A height profile taken along the line A-B is shown Fig. 2(b). Topographic height  $z$  measured at such a high negative voltage should closely follow the actual morphology, since the spectra of the occupied states were found to be nearly featureless. The steepest slope in  $z$  allows one to determine the positions of the SF steps,<sup>25</sup> which are indicated by the dashed lines in (a) [also in (c)–(h)] and by the downward arrows in (b). The straight SF lines and the threefold symmetry imposed by the film and the substrate lead to an ideally shaped equilateral triangle<sup>26</sup> where the quantum confinement of surface states is expected.<sup>27</sup> The presence of quantized states in the island and their evolution with increasing energy are demonstrated by  $dI/dV$  images in Figs. 2(c)–2(e) [(c)  $V=+0.09$  V, (d)  $V=+0.26$  V, and (e)  $V=+0.50$  V]. Here  $dI/dV$  signal was deconvoluted to recover a quantity proportional to the surface density of states  $\rho$  at a fixed height, according to the recipe prescribed by Li *et al.*<sup>25</sup> Referential topographic height needed for the deconvolution was obtained from Fig.

2(a). Figures 2(f)–2(h) show simulated  $dI/dV$  images based on the analytical solutions for an equilateral triangle with perfect confinement.<sup>28</sup> The excellent agreement between the experimental and simulated images demonstrates that such SF triangles are ideal electron resonators and can be utilized to investigate the intrinsic properties of the quantum confinement.

Reflection amplitudes at SF steps were determined by measuring the energy widths of quantized states in triangle resonators. This is based on the fact that electron lifetime  $\tau$ , relating to the energy width  $\Gamma$  through an equation  $\tau=\hbar/\Gamma$ , is limited by incomplete reflection at the boundary.<sup>14,17,18</sup> For the same effective radius  $S$  of the resonator and the same energy  $E$ , a larger  $\Gamma$  corresponds to a smaller reflection amplitude  $R$ . Here  $S$  is given by the radius of the largest enclosed circle for a noncircular resonator [see the inset of Figs. 2(i) and 2(j)].<sup>18,29</sup> Figure 2(i) shows a representative  $dI/dV$  spectrum (dots) taken on a triangle island bounded by descending SF (side length  $d=4.83$  nm,  $S=1.39$  nm). Three sharp peaks correspond to quantized states located at  $E=0.109$ ,  $0.264$ ,  $0.484$  eV. The spectrum was fitted using multiple Lorentzian functions to obtain the full width at half maximum  $\Gamma$  of each peak. For example, the peak width at  $E=0.484$  eV (peak  $\alpha$ ) was determined to be  $\Gamma=110\pm 14$  meV. Similar experiments were also performed on resonators bounded by MA steps for comparison. In this case, hexagons were chosen since they are commonly observed due to the sixfold symmetry of the Ag(111) surface. Figure 2(j) shows a  $dI/dV$  spectrum (dots) taken on a hexagonal island bounded by MA steps ( $d=1.80$  nm,  $S=1.56$  nm), which is similar in  $S$  to the triangle island. Although three peaks are likewise visible at  $E=0.134$ ,  $0.418$ ,  $0.763$  eV, they are obviously broader than those in Fig. 2(i). The same fitting analysis using multiple Lorentzians gives  $\Gamma=276\pm 30$  meV for  $E=0.418$  eV (peak  $\beta$ ), being much larger than that of peak  $\alpha$ . This indicates that the reflection amplitude is higher for SF steps than for MA steps.

We remark on some detailed aspects of our analysis. Although the peaks compared in the above are close in energy, they belong to different energy levels, i.e., the third lowest in Fig. 2(i) and the second lowest in Fig. 2(j). This is due to different shapes of resonators adopted for SF steps and MA steps. The eigenenergies of the quantum resonators surrounded by infinitely high-potential barriers are given as follows:

$$E_n = E_0 + \frac{\hbar^2 \pi^2}{2m^* S^2} A_n \quad (n = 1, 2, 3, \dots), \quad (1)$$

where  $A_n=0.444, 1.037, 1.778, \dots$  are for an equilateral triangle<sup>28</sup> and  $A_n=0.544, 1.377, 2.464, \dots$  for an equilateral hexagon ( $A_n$  were obtained numerically for the hexagon).  $E_0$  and  $m^*$  are the onset energy and the effective mass of the relevant energy band, respectively. We note that the effective radius  $S$  to be used here may deviate from the value determined from the topography of the island,  $S_{\text{topo}}$ . This is because electrons are not strictly confined within the step boundary in a real resonator, in contrast to the theoretical model. This is clearly visible from the experimental [Figs.

2(c)–2(e)] and simulated [Figs. 2(f)–2(h)]  $dI/dV$  images; the former has a larger area of high  $dI/dV$  signal than the latter for the same energy. Therefore, we determined an electronic effective radius  $S_{el}$  by comparing the three lowest peak energies of a spectrum to theoretical eigenenergies in Eq. (1). If one uses the effective mass of Ag(111) surface states  $m^* = 0.4m_0$  ( $m_0$ : free-electron mass),<sup>9,25</sup> one obtains  $S_{el} = 1.84 \pm 0.06$  nm for the SF triangle [Fig. 2(i)] and  $S_{el} = 1.69 \pm 0.03$  nm for the MA hexagon [Fig. 2(j)]. The former is larger than  $S_{topo} = 1.39$  nm while the latter is close to  $S_{topo} = 1.56$  nm. Furthermore, the same analysis also allows one to determine the band onset energy  $E_0$ . This gives  $E_0 = -0.022 \pm 0.019$  eV and  $E_0 = 0.020 \pm 0.060$  eV, respectively, which are in the order of the surface-state onset energy of Ag(111) films grown on Si substrates.<sup>30</sup> These values are higher than that of a bulk single crystal [−0.063–−0.065 eV (Refs. 9 and 31)] due to the in-plane tensile strain in the Ag films.<sup>30</sup> The variation in  $E_0$  for our samples suggests spatially inhomogeneous strains in the films, which may be caused by creation and annihilation of SF defects.

Reflection amplitude  $R$  was deduced from the peak width  $\Gamma$  as follows. First, the effects of thermal and instrumental broadenings were removed to extract the peak width  $\Gamma_{deconv}$  of a deconvoluted spectrum. Then a theoretical intrinsic energy width due to electron-electron and electron-phonon scattering (5–18 meV for  $E = 0.1$ –0.8 eV)<sup>32,33</sup> was subtracted from  $\Gamma_{deconv}$  to obtain the contribution from the boundary reflection  $\Gamma_R$ . Finally,  $R$  was calculated from  $\Gamma_R$  through the following equation:

$$\Gamma_R = -\frac{\hbar^2}{m^*} \sqrt{\frac{2m^*(E - E_0) \ln|R|}{\hbar^2 S}}, \quad (2)$$

where  $m^* = 0.4m_0$ ,  $E_0$  and  $S (= S_{el})$  being determined as described above. This analysis gives  $R = 0.67 \pm 0.04$  for the peak  $\alpha$  [Fig. 2(i)] and  $R = 0.32 \pm 0.03$  for the peak  $\beta$  [Fig. 2(j)], confirming the earlier argument. The same measurements were repeated on seven SF triangles and 13 MA hexagons with different sizes, and 54 peaks were analyzed in total. The results are summarized in Fig. 3 for SF steps (circles) and MA steps (squares). The closed and open circles represent data for descending and ascending steps, respectively.  $R$  at MA steps rapidly decreases from about 0.7 to 0.3 as  $E$  increases from 0 to 0.4 eV, which is in consistent with the previous report by Bürgi *et al.*<sup>9</sup> In clear contrast,  $R$  for SF steps maintains high values around 0.6–0.7 at least up to 0.5 eV. Our tight-binding calculations of reflection amplitude performed for both types of steps confirmed this finding. Black and gray lines in Fig. 3 show  $R$  calculated for SF and MA steps, respectively, the former being clearly higher than the latter (solid line: descending steps, dotted line: ascending steps). Interestingly, the result is against an intuitive expectation that a lower step height should result in a weaker electron reflection. This anomaly may be explained by the existence of the subsurface structures for SF steps as follows.

We first note that Shockley surface states on a noble metal generally extend over several atomic layers from the surface.<sup>1</sup> They extend more into the bulk region as the en-

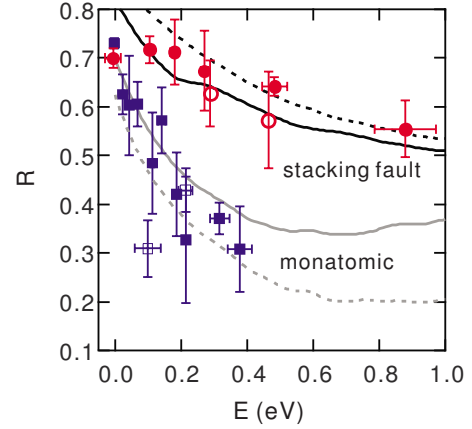


FIG. 3. (Color online) Reflection amplitudes  $R$  at SF steps (circles) and MA steps (squares) as a function of energy  $E$ . The black and gray lines show tight-binding calculations for SF steps and for MA steps, respectively. See the text for details.

ergy  $E$  increases from the band onset and almost become surface resonances around 1 eV.<sup>34</sup> Considering that a MA step is a surface-localized defect and retains the bulk periodicity below the surface, its reflection amplitude will decrease rapidly in this energy region. For example, in the case of Au(111) surfaces, the effective potential barrier height of a MA step is reduced to 10–20 % of the original value when the decay length  $\lambda$  of surface states increases to 9–20 ML.<sup>11</sup> The essentially same phenomenon is expected to occur for Ag(111) surfaces due to their similar electronic properties. In contrast, SF defects studied here extend to the bottom of the film because they are created by the substrate template. Although a SF surface step can only weakly reflect resonance-like surface states for the same reason, this does not apply to the subsurface part of the SF. Indeed, a strong anisotropic modulation of *bulk* quantum well states of Ag films by periodic SF planes has been found experimentally<sup>20,21</sup> and theoretically,<sup>23</sup> which means a strong reflection of bulk states by a SF plane. Therefore, surface states can be strongly reflected by the subsurface SF plane even if they penetrate deeply and approach resonance states at high energies.

In summary, we have demonstrated high reflection amplitudes at SF steps around 0.6–0.7 for  $E = 0$ –0.5 eV, unexpectedly higher than those for MA steps. The present result offers a promising route for effective electron confinement and fabrication of various quantum structures on metal surfaces. For example, quantum confinement of Ag(111) surface states within a terrace as narrow as 1.3 nm can be realized using SF steps.<sup>35</sup> Such well-defined 1D states might be used to mediate an anisotropic exchange interaction and to control spins of molecules line by line, which will be the subject of a forthcoming study.

We thank R. Berndt, J. Kröger, O. Groening, and S. Crampin for fruitful discussions and M. Becker for his technical support in the early stage. T.U. acknowledges JSPS for the financial support KAKENHI Grant No. 21510110 and Iketani Science and Technology Foundation.

\*uchihashi.takashi@nims.go.jp

- <sup>1</sup>A. Zangwill, *Physics at Surfaces* (Cambridge University Press, Cambridge, 1988), Chap. 4.
- <sup>2</sup>M. F. Crommie, C. P. Lutz, and D. M. Eigler, *Nature (London)* **363**, 524 (1993).
- <sup>3</sup>Y. Hasegawa and Ph. Avouris, *Phys. Rev. Lett.* **71**, 1071 (1993).
- <sup>4</sup>F. Silly, M. Pivetta, M. Ternes, F. Patthey, J. P. Pelz, and W.-D. Schneider, *Phys. Rev. Lett.* **92**, 016101 (2004).
- <sup>5</sup>Y. Pennec, W. Auwärter, A. Schiffrin, A. Weber-Bargioni, A. Riemann, and J. V. Barth, *Nat. Nanotechnol.* **2**, 99 (2007).
- <sup>6</sup>G. Schull, M. Becker, and R. Berndt, *Phys. Rev. Lett.* **101**, 136801 (2008).
- <sup>7</sup>Ph. Avouris and I.-W. Lyo, *Science* **264**, 942 (1994).
- <sup>8</sup>J. Li, W.-D. Schneider, R. Berndt, and S. Crampin, *Phys. Rev. Lett.* **80**, 3332 (1998).
- <sup>9</sup>L. Bürgi, O. Jeandupeux, A. Hirstein, H. Brune, and K. Kern, *Phys. Rev. Lett.* **81**, 5370 (1998).
- <sup>10</sup>A. Mugarza, A. Mascaraque, V. Pérez-Dieste, V. Repain, S. Rousset, F. J. García de Abajo, and J. E. Ortega, *Phys. Rev. Lett.* **87**, 107601 (2001).
- <sup>11</sup>A. Mugarza and J. E. Ortega, *J. Phys.: Condens. Matter* **15**, S3281 (2003).
- <sup>12</sup>K. Morgenstern, K.-F. Braun, and K.-H. Rieder, *Phys. Rev. Lett.* **89**, 226801 (2002).
- <sup>13</sup>M. F. Crommie, C. P. Lutz, and D. M. Eigler, *Science* **262**, 218 (1993).
- <sup>14</sup>J. Kliewer, R. Berndt, and S. Crampin, *New J. Phys.* **3**, 22 (2001).
- <sup>15</sup>E. J. Heller, M. F. Crommie, C. P. Lutz, and D. M. Eigler, *Nature (London)* **369**, 464 (1994).
- <sup>16</sup>G. Hörmandinger and J. B. Pendry, *Phys. Rev. B* **50**, 18607 (1994).
- <sup>17</sup>H. Jensen, J. Kröger, R. Berndt, and S. Crampin, *Phys. Rev. B* **71**, 155417 (2005).
- <sup>18</sup>S. Crampin, H. Jensen, J. Kröger, L. Limot, and R. Berndt, *Phys. Rev. B* **72**, 035443 (2005).
- <sup>19</sup>C. Tournier-Colletta, B. Kierren, Y. Fagot-Revurat, and D. Malterre, *Phys. Rev. Lett.* **104**, 016802 (2010).
- <sup>20</sup>N. Nagamura, I. Matsuda, N. Miyata, T. Hirahara, S. Hasegawa, and T. Uchihashi, *Phys. Rev. Lett.* **96**, 256801 (2006).
- <sup>21</sup>T. Okuda, Y. Takeichi, K. He, A. Harasawa, A. Kakizaki, and I. Matsuda, *Phys. Rev. B* **80**, 113409 (2009).
- <sup>22</sup>K. Sawa, Y. Aoki, and H. Hirayama, *Phys. Rev. Lett.* **104**, 016806 (2010).
- <sup>23</sup>K. Kobayashi and T. Uchihashi, *Phys. Rev. B* **81**, 155418 (2010).
- <sup>24</sup>T. Uchihashi, C. Ohbuchi, S. Tsukamoto, and T. Nakayama, *Phys. Rev. Lett.* **96**, 136104 (2006).
- <sup>25</sup>J. Li, W.-D. Schneider, and R. Berndt, *Phys. Rev. B* **56**, 7656 (1997).
- <sup>26</sup>The detailed mechanism of the SF triangle creation is not clear, but a likely scenario is as follows. First, three stacking-fault planes with different orientations are created at the film-substrate interface due to triple domains of In  $4 \times 1$ . Then they penetrate the film and meet in close proximity to one another at the surface.
- <sup>27</sup>K. Kanisawa, M. J. Butcher, Y. Tokura, H. Yamaguchi, and Y. Hirayama, *Phys. Rev. Lett.* **87**, 196804 (2001).
- <sup>28</sup>H. R. Krishnamurthy, H. S. Mani, and H. C. Verma, *J. Phys. A* **15**, 2131 (1982); T. Kumagai and A. Tamura, *J. Phys. Soc. Jpn.* **77**, 014601 (2008).
- <sup>29</sup>The validity of the effective radius  $S$  is independent of the symmetry of the state (A1 symmetry or non-A1 symmetry) at least for the lowest few states, although only A1 symmetry states were discussed in Ref. 18 [S. Crampin (private communication)].
- <sup>30</sup>G. Neuhold and K. Horn, *Phys. Rev. Lett.* **78**, 1327 (1997).
- <sup>31</sup>M. Pivetta, F. Silly, F. Patthey, J. P. Pelz, and W.-D. Schneider, *Phys. Rev. B* **67**, 193402 (2003).
- <sup>32</sup>A. Eiguren, B. Hellsing, F. Reinert, G. Nicolay, E. V. Chulkov, V. M. Silkin, S. Hüfner, and P. M. Echenique, *Phys. Rev. Lett.* **88**, 066805 (2002); L. Vitali, P. Wahl, M. A. Schneider, K. Kern, V. M. Silkin, E. V. Chulkov, and P. M. Echenique, *Surf. Sci.* **523**, L47 (2003).
- <sup>33</sup>O. Jeandupeux, L. Bürgi, A. Hirstein, H. Brune, and K. Kern, *Phys. Rev. B* **59**, 15926 (1999); L. Bürgi, O. Jeandupeux, H. Brune, and K. Kern, *Phys. Rev. Lett.* **82**, 4516 (1999).
- <sup>34</sup>M. Becker, S. Crampin, and R. Berndt, *Phys. Rev. B* **73**, 081402(R) (2006).
- <sup>35</sup>T. Uchihashi, K. Kobayashi, and T. Nakayama (unpublished).